ACS APPLIED MATERIALS & INTERFACES

Research Article

www.acsami.org

High Ferromagnetic Transition Temperature in PbS and PbS:Mn Nanowires

Swapan K. Mandal,*[,†] Arup Ratan Mandal,[†] and Sangam Banerjee[‡]

[†]Department of Physics, Visva-Bharati, Santiniketan, 731 235, India

[‡]Surface Physics Division, Saha Institute of Nuclear Physics, 1/AF Bidhannagar, Kolkata, 700 064, India

ABSTRACT: Spontaneous magnetization measured in the temperature range 5−300 K with high ferromagnetic transition temperature (T_c) has been observed in both undoped and Mn doped (2−8 mol %) PbS nanowires (diameter 30 nm) in polymer. For undoped sample, we find $T_c \sim 290$ K while for doped samples T_c varies between 310−340 K depending on Mn concentrations. Both T_c and coercive fields are critically dependent on Mn concentrations. Coercive fields show a $T^{0.5}$ dependence with temperature for a moderate concentration of Mn (4 mol %) in PbS while it deviates from $T^{0.5}$ behavior for higher Mn concentrations. Anionic defects arising out of nonstoichiometric growth is solely responsible for the observed magnetism in undoped PbS nanowires. The role of intrinsic strain along with reduced dimensionality in determining such high T_c and overall magnetizations has been discussed.

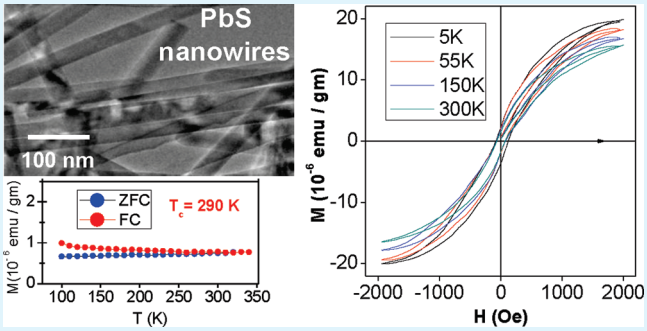

KEYWORDS: *magnetic semiconductor, ferromagnetism, PbS, nanowires, strain, defects*

1. INTRODUCTION

Nanoscale magnetism plays an increasingly important role in next-generation magnetic storage devices and microelectronic industries. The magnetic properties of materials with nanometric dimensions differ from those of macroscopic samples (bulk) because of broken translational symmetry, appearance of higher proportion of atoms in the surface, surface anisotropy and also from the fact that sizes of the nanoscale objects become comparable to some fundamental or characteristic lengths like exchange length, domain wall width etc. of the constituent materials.[1,2] In the case of magnetic nanoparticles, a single domain configuration is energetically more favorable, whereas for materials with microscopic or macroscopic sizes the lowest energy configuration shifts to an arrangement with more than one magnetic domain. The dynamical behaviors of such magnetic nanoparticles are also largely influenced by thermal fluctuations, surroundings and other effects. Another important aspect is the doping of such magnetic nanomaterials by the other elements that may give rise to remarkable properties compared to the bulk and is a subject of intense research in recent years.[3] One interesting area of looking into the effect of doping in magnetic materials is the synthesis of diluted magnetic semiconductors (DMSs).[4−6]

DMSs have been the focus of intense research today for the realization spin-based electronic devices.[4−7] Traditionally, such a DMS is generally fabricated from suitably doped (by 3d transition metals or 4f rare-earth ions) II−VI or IV−VI semiconductors either in bulk or in low-dimensional form. The interaction between 3d electrons of doped element and s or p itinerant carriers of the host semiconductor is believed to be responsible for the appearance of ferromagnetism. Application of external magnetic field or temperature to the system may perturb the above sp−d interaction and plausibly gives rise to interesting electronic or magnetic properties. However, despite of a large number of studies to date, the realization of prototype spin-based devices is hindered mainly because of low T_c in such DMSs. On the other hand, a consensus view on the observed ferromagnetism to be intrinsic or extrinsic in origin is still lacking. Interestingly, ferromagnetism has also been observed in undoped wide band gap oxide semiconductor nanostructures, which is attributed either to the reduced dimensionality of the system or intrinsic defects or both.[8−10] Low-dimensional semiconductor nanostructures are associated with large surface area grain boundaries and structural deviations from perfect crystallinity. This further leads to minute or severe deviation from stoichiometric growth of nanocrystals depending on the material fabrication process. Nonstoichiometry in crystals results the formation of large concentration defects or vacancies which is attributed to a plausible source of generating local magnetic moments and collectively leads to the appearance of ferromagnetism in materials which is otherwise nonmagnetic in nature.[11] The defect induced ferromagnetism is now supported by many experimental evidence mainly in oxide nanostructures[8−12] and is believed to be purely intrinsic. Besides defects, the growth of nanostructures is also associated with inhomogeneous lattice strain within the crystal which is very

Received: September 17, 2011
Accepted: December 5, 2011
Published: December 5, 2011

crucial in governing many important electronic properties in semiconducting systems. The strain may intrinsically present in nanostructures as a result of reduced dimension of the system. However, the effect of such intrinsic strain on the magnetic properties in DMS system is hardly explored.[13] The inhomogeneous strain can increase the crystal's internal energy and can locally modify the magnetic anisotropy which in turn can significantly increase the ferromagnetic transition temperature (T_c) and may be quite important in understanding the high T_c magnetic semiconductors.

In this report, we primarily investigate with experimental evidence three important issues concerned with the ferromagnetism: (i) nonstoichiometry, (ii) reduced dimensionality and (iii) intrinsic strain. Various doped semiconducting nanowires are found to exhibit ferromagnetism with a Curie temperature around 300 K.[14−18] For this purpose, we synthesized both undoped and Mn-doped PbS nanowires stabilized by a polymer. Interestingly, we find that both undoped and Mn-doped PbS show ferromagnetism near and above room temperature and make a comprehensive analysis on the effect of Mn concentration on the ferromagnetic behaviors of PbS nanowires.

2. EXPERIMENTAL SECTION

Preparation of PbS Nanowires. Synthesis of PbS and PbS:Mn nanowires is accomplished by a simple wet chemical route. The details of synthesis (also structural and microscopic characterizations) have been reported in details elsewhere.[19,20] Briefly, the process involves exchange of Pb^{2+} ions in the pyrrole and then reacting with S^{2-} ions. $Pb(NO_3)_2$ and $Na_2S_2O_3$, $5H_2O$ (purified) are used for Pb^{2+} and S^{2-} precursors, respectively. Ethanol dried over activated molecular sieve zeolite 4A and distilled water is used as the solvent (ethanol: water = 1:5) keeping at a bath temperature of 60 °C. Before reactions, both lead and sulfur solutions are continuously stirred for two hours keeping the bath temperature same 60 °C. When sulfur solution is slowly added to the lead solution, PbS is immediately formed within polypyrrole matrix. The precipitate is washed in distilled water three times, filtered and dried at room temperature in vacuum. Mn doping is done by replacing Pb^{2+} with different molar percentage of Mn^{2+} (using $Mn(CH_3COO)_2$, $4H_2O$ as the precursor) in the lead solution. For the present study, we are concerned with five samples, undoped PbS (S-1) and Mn doped PbS nanowires (S-2 to S-5) in polypyrrole (5 wt %). The molar % of Mn in S-2, S-3, S-4, and S-5 are 2, 4, 6, and 8, respectively.

Characterization. Morphology and crystal structure of the nanowires are investigated by using a transmission electron microscope (TEM, JEOL) and an X-ray diffractometer (XRD, Philips) respectively. Magnetization measurements are performed using a commercial superconducting quantum interference device (SQUID) magnetometer (MPMS-7, Quantum Design).[7] X-ray photoelectron spectroscopic (XPS) measurement is carried out by SPECS, Germany with a resolution of 1400 kcps, and using Mg K_α radiation with Mg anode at 300 W at a base pressure ~2 × 10^{-9} Torr. Electron paramagnetic resonance (EPR) data are recorded at 9.833 GHz with a Bruker BioSpin GmbH spectrometer.

3. RESULTS AND DISCUSSION

Figure 1 shows the TEM image of a representative sample S-1, where the average size (diameter) of the nanowires is obtained about 30 nm and does not show any significant change in their size and distribution upon Mn doping. We have also observed that both PbS and PbS:Mn nanowires in polymer suffer a strain during their growth and is influenced by the Mn concentrations too. Such a strain is manifested in resulting significant deviations in peak positions and their distribution in intensity from the bulk fcc PbS lattice as revealed by the X-ray diffraction

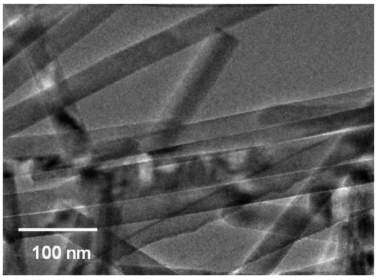

Figure 1. Transmission electron microscope (TEM) image PbS nanowires (sample S-1) showing the formation of nanowires of average size about 30 nm.

(XRD) spectra, details of which are given in ref 19. The bulk cubic lattice of sites $a = b = c = 5.9413$ Å (Figure 2a) is found to

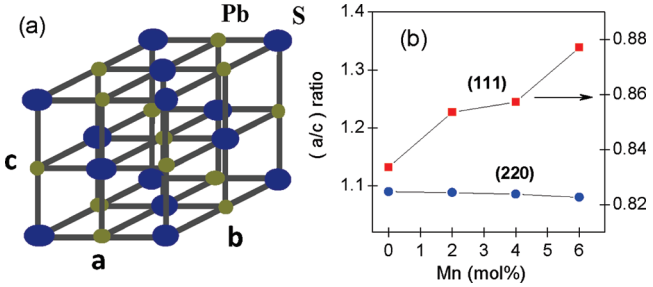

Figure 2. (a) Schematic diagram of a bulk PbS lattice of sites (a , b, c) where $a = b = c$. (b) Plot of the ratio a/c for PbS nanowires with various Mn concentrations.

be distorted resulting into a tetragonal lattice structure for the PbS nanowires in polymer. Considering the most intense (220) and (111) reflections, we plot the a/c ratio for various Mn concentrations in Figure 2b. The data reveal that the lattice suffers both compressive as well as expansive strain, which is inherent to the growth process itself and influenced by Mn doping that subsequently plays an important role in determining the magnetic properties of PbS and PbS:Mn nanowires as discussed below.

To unveil the magnetic properties, first we present the typical hysteresis curves showing the plot of magnetization (M) vs magnetic field (H) for all the samples in Figure 3a−e. The data are recorded for each sample up to 2000 Oe at four different temperatures 5, 55, 150, and 300 K respectively. The data clearly shows the distinct spontaneous magnetization (M_s) behaviors for both undoped and Mn-doped PbS nanowires at all given temperatures indicating the presence of ferromagnetic order. The most notable result is the observation of room temperature ferromagnetism in intrinsic (undoped) PbS nanowires. The hysteresis curves also show that the coercive field (H_c) and saturation magnetization (M_s) are dependent on the Mn concentration and the temperature of measurement for all the samples. H_c sharply increases with incorporation of Mn up to 4% and then decreases with further increase of Mn concentration in PbS lattice as can be seen from Figure 4a. On the other hand, H_c is found to increase with the reduction in temperature and is delineated as a function of square toot of temperature ($T^{0.5}$) in Figure 4b. The data shows that for samples S-2 and S-3, H_c varies well as a function of square root of temperature. However, the data deviates from $T^{0.5}$ behavior in the observed temperature range when the Mn concentration in the sample is relatively high (sample S-4 and S-5) because of

dx.doi.org/10.1021/am201261v | ACS Appl. Mater. Interfaces 2012, 4, 205−209

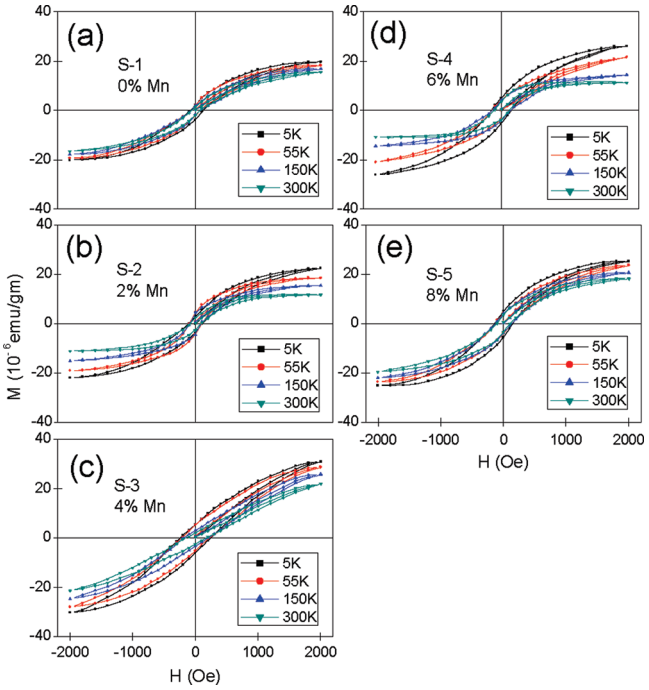

Figure 3. Hysteresis loops (M vs H) of PbS naowires measured at T = 5, 55, 150, and 300 K with various Mn mol % concentrations (a) 0, (b) 2, (c) 4, (d) 6, and (e) 8.

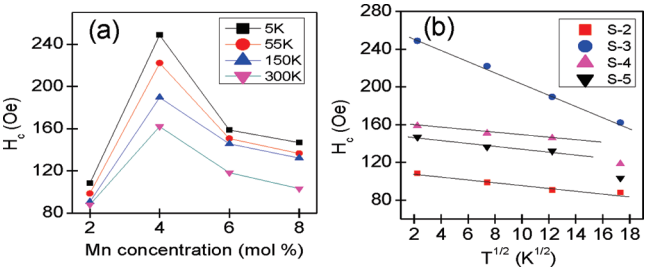

Figure 4. (a) Variation in coercive field (H_c) obtained for PbS nanowires with Mn concentrations obtained at different temperatures. (b) Variation in H_c with temperature (T) obtained for samples with different Mn concentrations.

Mn clustering at the surface as discussed later. Similar $T^{0.5}$ dependence of coercivity is observed for Mn doped ZnS nanocrystals[21] and is largely expected for noninteracting ferromagnetic systems.[22,23]

In Figure 5a–e, we present the zero-field-cooled (ZFC) and field-cooled (FC) (100 Oe) magnetization curves for all the samples. Figure 5 reveals the distinct bifurcation of ZFC and FC curves at finite temperatures (T_c) for all the samples. T_c corresponds to 290 K for the undoped sample S-1 and that for S-2 (2% Mn) and S-3 (4% Mn) at 310 and 340 K, respectively. T_c is found to decrease with further increase in Mn concentrations and is measured to be 330 and 322 K for S-4 (6% Mn) and S-5 (8% Mn), respectively. The increase in T_c with the increase in spin magnetic moments is consistent with the fact that more thermal energy is needed to randomize the magnetic ordering. However, why the T_c values are so high in such low-dimensional nanowires compared to its bulk needs to be discussed and may have significant implications in the study of diluted magnetic semiconductors.

Now, we discuss the origin of ferromagnetism in both undoped and Mn doped PbS nanowires. IV–VI semi-

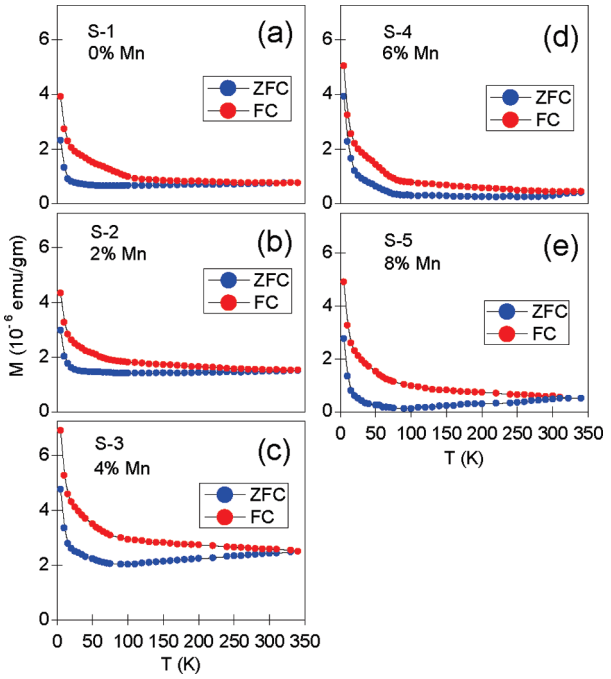

Figure 5. ZFC and FC magnetization curves (M vs T) of PbS nanowires plotted for various Mn mol % concentrations (a) 0, (b) 2, (c) 4, (d) 6, and (e) 8. The data shows the distinct bifurcation of the ZFC and FC curves in the temperature range 290–340 K.

conductors like PbS are found to have a concentration of native defects (1×10^{17} to 1×10^{21} cm^{-3}) because of their intrinsic tendency to grow nonstoichiometrically.[24,25] An excess of Pb results in n-type conductivity in PbS, whereas an excess of S makes it p-type.[26] In our case, the samples are presumably assumed to be n-type following the Pb:S ratio to be ~1.02:1 (obtained from X-ray photoelectron spectroscopy and energy-dispersive X-ray data), deviating slightly from its stoichiometric composition. The ground-state configuration of sulfur is [Ne] $3s^2 3p^4$. According to Hund's rule, the p orbitals must fill up separately first. This results in the first 3 electrons going into separate orbitals, and the fourth then doubles up with the first, leaving the other two p orbitals with unpaired electrons. The 3p sulfur vacancies are supposed to give rise the magnetic moments for the observed ferromagnetism in undoped nanowires. However, the exact nature of correlations or interactions among the vacancies is not known to us. Another important aspect may be relevant to discuss the enhancement of magnetic moments due to oxygen doping.[16] Growth of PbS nanocrystals may accompany oxygen as a codopant, particularly at the surface, unless specific measures are taken to prevent it.[27] In our case, the possibility of surface oxidation is very low because the PbS nanowires are encapsulated in polymer and are not subjected to any high temperature during synthesis. We also did not detect any oxide phases of lead or manganese by XRD. So the enhancement of ferromagnetism due to the presence of oxygen may not be relevant in this investigation.

Intentional doping by magnetic impurity Mn in such PbS nanowires significantly modifies the interactions between localized Mn spins and itinerant carriers. The electronic state of doped Mn ions is confirmed to be Mn^{2+} by EPR investigations discussed later.[28] The Mn^{2+} resides preferentially in the substitutional sites of Pb^{2+} in the PbS lattice causing no appreciable distortion of the host lattice as proved by the XRD

dx.doi.org/10.1021/am201261v | ACS Appl. Mater. Interfaces 2012, 4, 205–209

spectra. Any isolated or uncoupled d-ions are quite unlikely to contribute to the ferromagnetism. A Mn^{2+} ion has d-electrons with total spin $S = 5/2$, $L = 0$ by Hund's rule and a magnetic moment of 5 μ_B. Coupling of d electrons with the itinerant carriers is responsible for the observed ferromagnetism in Mn doped PbS nanowires.[4−6,29] The coupling seems to be weak, which makes the carriers less localized within crystal volume giving rise to long-range ferromagnetic interactions even at room temperature. There exists a critical dilute Mn concentration (4 mol %), beyond which the magnetization is found to be decreased with a sharp reduction in coercive fields for all the samples. The reason could be the presence of antiferromagnetic interactions which becomes quite appreciable with large Mn concentrations due to nearest neighbor Mn−Mn antiferromagnetic exchange coupling, as observed for many low dimensional Mn doped systems.[14,21] To elucidate further on this issue, we address the dependence of T_c on Mn doping concentrations. ZFC-FC curves clearly reveal the T_c to sharply increase from 290 to 340 K as Mn concentration increases from 2 to 4% and any further attempt to increase the doping concentration results in the decrease in T_c values. We have observed that increase in Mn doping concentrations leads to Mn clustering at the nanowire surface. The surface spins may not align ferromagnetically to that of in the core of the nanowires and may lead to an overall decrease in magnetization of the samples. Such a behavior of the surface magnetic spins different from that of the core is observed for various magnetic semiconductor nanostructures.[30,31]

To look further on the antiferromagnetic exchange interactions between the Mn ions at higher concentrations, we present the EPR spectra (at room temperature) of two representative samples S-3 and S-5 respectively as shown in Figure 6. The magnetization data shows predominant

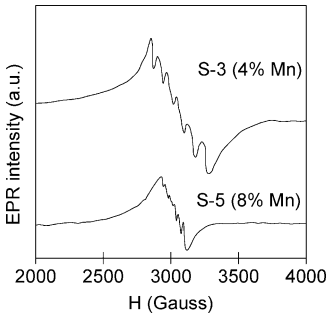

Figure 6. EPR spectra of Mn-doped PbS nanowires recorded at room temperature.

ferromagnetic ordering in S-3, whereas a fraction of doped Mn^{2+} ions in S-5 shows antiferromagnetic couplings. Typical six-line hyperfine spilt structures can be observed for S-3 (4% Mn) corresponding to some isolated Mn^{2+} ions arising out of $|-1/2\rangle$to $|1/2\rangle$transition coupled to nuclear spin of Mn ($I = 5/2$). Increase in Mn concentration (8%) as the case for sample S-5 results into a EPR spectrum with reduced intensity and nearly unresolved hyperfine lines. This clearly reveals the presence of antiferromagnetic interaction between the Mn ions with the increase in Mn concentrations and is found to be observed for many Mn doped semiconducting systems.[21,32] Thus the EPR spectra clearly uphold the magnetic behaviors of Mn doped PbS nanowires as obtained from SQUID data discussed above. We also find that there is a significant shift of the resonance field to lower value with the increase in Mn concentration. The resonance fields are obtained about 3064 and 3024 G for samples S-3 and S-5, respectively. Such a shift (40 G) is ascribed to the polarization of free carriers by Mn ions in presence of local magnetic field.[28,33] This further confirms the interaction of free carrier spins with Mn^{2+} magnetic moments in Mn-doped samples negating the possibility of magnetization solely due to defects as observed for undoped PbS nanowires. Nonetheless, we believe that more independent measurements like exchange bias effect may further clarify the issue.[34]

Finally, we address the issue of high Curie temperature in such fine PbS nanowires in contrast to its bulk values. High T_c values in many narrow and high band gap semiconducting nanowires are found experimentally although theoretical predictions based on electronic structure calculations are much lower than the experimental values. Sometimes combination of electronic structure calculations with percolation models gives better results but not in exact commensuration with the experimental results.[35] Here, we provide a qualitative discussions on this aspect which can make sense of achieving such high values of T_c. We have observed that all the as-grown PbS nanowires in polymer suffer inhomogeneous strain in their tetragonal crystal lattice structures. Apart from the inherent strain, substitution of Pb^{2+} in Mn^{2+} in the PbS lattice may further introduce much local strain due to their difference in ionic radii. The ionic radius of Pb (1.19 Å) is nearly 2.6 times larger than that of doped Mn ions (0.46 Å). This inhomogeneous strain in the samples and the local distortion of the lattice around the doped magnetic centers increases the crystal's internal energy which can largely shift the ferromagnetic transition temperature. The change in lattice parameters due to strain results change in primitive cell volume (and thus in anisotropy) and in turn can change the transition temperature as evidenced by many experiments.[36,37] Recently, Xu et al.[37] observed an increase in T_c for MnAs/GaAs layer as a result of stretching of lattice parameters in the basal plane or compressing of lattice parameter in the perpendicular direction. Although the exact relationship between the strain and the transition temperature are not yet properly established, it opens a new possibility to control the magnetic properties through strain parameters, which may be useful for future spintronic applications.

4. CONCLUSIONS

In conclusion, we report here the experimental observations of ferromagnetism with high T_c in both intrinsic and magnetically doped PbS nanowires in polymer. Defects due to anionic vacancies arising out of nonstoichiometry in composition plausibly give rise to ferromagnetism in undoped sample at 290 K. The T_c values are found to increase upon Mn doping until 4 mol % above which it is found to be reduced. The reduction in T_c with 6−8 mol % Mn concentration is attributed to the Mn clustering at the surface which may couple antiferromagnetically to the core magnetic moments. The coercivity is found to follow $T^{0.5}$ dependence with temperature for moderate concentration of Mn up to 4%. The intrinsic strain and the reduced dimensionality of the system play crucial role in determining high values of T_c and are quite important toward realization of spintronic devices.

AUTHOR INFORMATION

Corresponding Author

*Tel: +91 3463-261016. E-mail: sk_mandal@hotmail.com.

■ ACKNOWLEDGMENTS

This work was partially supported by CSIR, Government of India, New Delhi.

■ REFERENCES

(1) Dormann, J. L.; Fiorani, D. *Magnetic Properties of Fine Particles*; North-Holland: Amsterdam, 1992.
(2) Gubin, S. P.; Koksharov, Y. A; Khomutov, G. B.; Yurkov, G. Y. *Russ. Chem. Rev.* **2005**, *74*, 489−520.
(3) Chambers, S. A.; Droubay, T. C.; Wang, C. M.; Rosso, K. M.; Heald, S. M.; Schwartz, D. A.; Kittilstved, K. R.; Gamelin, D. R. *Mater. Today* **2006**, *9*, 28−35.
(4) Dietl, T.; Ohno, H.; Matsukura, F.; Cibert, J.; Ferrand, D. *Science* **2000**, *287*, 1019−1022.
(5) König, J.; Lin, H. H.; MacDonald, A. H. *Phys. Rev. Lett.* **2000**, *84*, 5628−5631.
(6) Coey, J. M. D.; Venkatesan, M.; Fitzgerald, C. B. *Nat. Mater.* **2005**, *4*, 173−179.
(7) Banerjee, S.; Mandal, M.; Gayathri, N.; Sardar, M. *Appl. Phys. Lett.* **2007**, *91*, 182501−1−182501−3.
(8) Dev, P.; Xue, Y.; Zhang, P. *Phys. Rev. Lett.* **2008**, *100*, 117204−1−117204−4.
(9) Sundaresan, A.; Bhargavi, R.; Rangarajan, N.; Siddesh, U.; Rao, C. N. R. *Phys. Rev. B* **2006**, *74*, 161306R-1−161306R-4.
(10) Osorio-Guillén, J.; Lany, S.; Barabash, S. V.; Zunger, A. 2007 *Phys. Rev. B* **2007**, *75*, 184421−1−184421−9.
(11) Tachiki, M.; Dunlap, B. D.; Crabtree, G. W. *Phys. Rev. B* **1983**, *28*, 5342−5344.
(12) Wu, J.; Mao, S.; Ye, Z. -G.; Xie, Z.; Zheng, L. *ACS. Appl. Mater. Interface* **2010**, *2*, 1561−1564.
(13) Kazakova, O.; Kulkarni, J. S.; Holmes, J. D.; Demokritov, S. O. *Phys. Rev. B* **2005**, *72*, 094415−1−094415−6.
(14) Delikanli, S.; He, S.; Qin, Y.; Zhang, P.; Zeng, H.; Zhang, H.; Swihart, M. *Appl. Phys. Lett.* **2008**, *93*, 132501−1−132501−3.
(15) Liu, B.; Bando, Y.; Tang, C.; Golberg, D.; Yamaura, K.; Muromachi, E. T. *Chem. Phys. Lett.* **2005**, *405*, 127−130.
(16) Kong, K. J.; Jung, C. S.; Jung., G. B.; Cho, Y. J.; Kim, H. S.; Park, J.; Yu, N. E.; Kang, C. *Nanotechnology* **2010**, *21*, 435703−1−435703−7.
(17) Wu, J. J.; Liu, S. C.; Yang, M. H. *Appl. Phys. Lett.* **2004**, *85*, 1027−1029.
(18) Arauio, C. M.; Kapilashrami, M.; Jun, X.; Jayakumar, O. D.; Nagar, S.; Wu, Y.; Arhammar, C.; Johansson, B.; Belova, L.; Ahuja, R.; Gehring, G. A.; Rao, K. V. *Appl. Phys. Lett.* **2010**, *96*, 232505−1−232505−3.
(19) Mandal, A. R.; Mandal, S. K. *J. Exp. Nanosci.* **2007**, *2*, 257−267.
(20) Mandal, S. K.; Mandal, A. R.; Barman, A.; Gautam, U. *J. Nanosci. Nanotechnol.* **2011**, *11*, 10234−10239.
(21) Sarkar, I.; Sanyal, M. K.; Kar, S.; Biswas, S.; Banerjee, S.; Chaudhuri, S.; Takeyama, S.; Mino, H.; Komori, F. *Phys. Rev. B* **2007**, *75*, 224409−1−224409−5.
(22) Lippens, P. E.; Lannoo, M. *Phys. Rev. B* **1989**, *39*, 10935−10942.
(23) Zeng, H.; Skomski, R.; Menon, L.; Liu, Y.; Bandyopadhyay, S.; Selimyer, D. J. *Phys. Rev. B* **2002**, *65*, 134426−1−134426−8.
(24) Allgaier, R. S.; Scanlon, W. W. *Phys. Rev.* **1958**, *111*, 1029−1037.
(25) Story, T.; Eggenkamp, P. J. T.; Swüste, C. H. W.; Swagten, H. J. M.; de Jonge, W. J. M.; Szczerbakow, A. *Phys. Rev. B* **1993**, *47*, 227−236.
(26) Scanlon, W. W. *Phys. Rev. B* **1953**, *92*, 1573−1575.
(27) Moody, I. S.; Stonas, A. R.; Lonergan, M. C. *J. Phys. Chem. C* **2008**, *112*, 19383−19389.
(28) Pifer, J. H. *Phys. Rev.* **1967**, *157*, 272−276.
(29) Gorska, M.; Anderson, J. R. *Phys. Rev. B* **1988**, *38*, 9120−9126.
(30) Chakrabarti, S.; Mandal, S. K.; Nath, B. K.; Das, D.; Ganguli, D.; Chaudhuri, S. *Eur. Phys. J. B* **2003**, *34*, 163−171.
(31) Barry, L.; Holmes, J. D.; Otway, D. J.; Copley, M. P.; Kazakova, O.; Morris, M. A. *J. Phys.: Cond. Matter* **2010**, *22*, 076001−1−076001−7.
(32) Story, T.; Eggenkamp, P. J. T.; Swüste, C. H. W.; Swagten, H. J. M.; de Jonge, W. J. M.; Szczerbakow, A. *Phys. Rev. B* **1993**, *47*, 227−235.
(33) Ben Mahmoud, A.; von Bardeleben, H. J.; Cantin, J. L.; Chikoidze, E.; Dumont, Y.; Mauger, A. *J. Appl. Phys.* **2007**, *101*, 09H102−1−09H102−3.
(34) Volobuev, V. V.; Stetsenko, A. N.; Sipatov, A. Y.; van Lierop, J. *Phys. Rev. B* **2010**, *81*, 134430−1−134430−7.
(35) Park, Y. D.; Hanbicki, A. T.; Erwin, S. C.; Hellberg, C. S.; Sullivan, J. M.; Mattson, J. E.; Ambrose, T. F.; Wilson, A.; Spanos, G.; Jonker, B. T. *Science* **2002**, *295*, 651−654.
(36) Seo, S. H.; Kang, H. C.; Jang., H. W.; Noh, D. Y. *Phys. Rev. B* **2005**, *71*, 012412−1−012412−3.
(37) Xu, P.; Lu., J.; Chen, L.; Yan, S.; Meng, H.; Pan, G.; Zhao, J. *Nanoscale Res. Lett.* **2011**, *6*, 125−131.